

## Prefactors for interlayer diffusion on Ag/Ag(111)

This article has been downloaded from IOPscience. Please scroll down to see the full text article.

2003 J. Phys.: Condens. Matter 15 5223

(<http://iopscience.iop.org/0953-8984/15/30/304>)

View [the table of contents for this issue](#), or go to the [journal homepage](#) for more

Download details:

IP Address: 171.66.16.121

The article was downloaded on 19/05/2010 at 14:22

Please note that [terms and conditions apply](#).

## Prefactors for interlayer diffusion on Ag/Ag(111)

Z Chvoj<sup>1,4</sup>, C Ghosh<sup>2</sup>, T S Rahman<sup>2</sup> and M C Tringides<sup>3</sup>

<sup>1</sup> Institute of Physics, Academy of Sciences of the Czech Republic, Na Slovance 2,  
182 21 Prague 8, Czech Republic

<sup>2</sup> Department of Physics, Cardwell Hall, Kansas State University, Manhattan, KS 66506, USA

<sup>3</sup> Department of Physics, Iowa State University, Ames, IA 50011, USA

E-mail: chvoj@fzu.cz

Received 20 February 2003

Published 18 July 2003

Online at [stacks.iop.org/JPhysCM/15/5223](http://stacks.iop.org/JPhysCM/15/5223)

### Abstract

Interlayer diffusion controls the transfer of atoms between layers in a film and is the key factor determining whether growth is layer-by-layer or two-dimensional. Analysis of recent experimental data on Ag/Ag(111) taken at two sets of temperatures provides similar values for the step edge barrier  $\Delta E_s$  but not for the ratio of the prefactors  $\nu_s/\nu_t$  where  $\nu_t$  is the prefactor for diffusion on a terrace and  $\nu_s$  the prefactor at a step edge site. A prefactor ratio larger than 1,  $\nu_s/\nu_t > 1$ , is extracted from the measurements at low temperature ( $T < 150$  K), while  $\nu_s/\nu_t \sim 1$  is found in the experiments done at a higher temperature ( $T \sim 300$  K). Since the conclusion  $\nu_s/\nu_t \sim 1$  is based on a steady state analysis of island decay, we examine whether this condition is fulfilled for Ag/Ag(111). We show that the low value of the terrace diffusion barrier on Ag(111) ( $E_t \approx 0.1$  eV) offers an alternative interpretation to the steady state analysis, i.e. an independent detachment model. Alternatively, we propose an independent detachment model. Re-analysis of the data in terms of this model results also in  $\nu_s/\nu_t > 1$ , in good agreement with the low temperature experiments.

### 1. Introduction

The interlayer probability for an atom encountering a step, to hop from a higher to a lower level, plays a decisive role in determining the type of growth mode observed in the system [1]. A strong step edge barrier (and therefore a low interlayer probability) is commonly assumed to be the reason for three-dimensional growth mode. This is the case for Ag/Ag(111) [2–4], which is the subject of this paper. Usually the probability  $p$  of interlayer diffusion is described by an Arrhenius form

$$p = (\nu_s/\nu_t) \exp(-\Delta E_s/kT), \quad (1)$$

<sup>4</sup> Author to whom any correspondence should be addressed.

where  $\nu_s$  is prefactor at the step edge,  $\nu_t$  the prefactor on the terrace,  $\Delta E_s$  is the step edge barrier,  $k$  is Boltzmann constant and  $T$  is temperature. Several methods have been applied with different experimental techniques (e.g. STM and diffraction) and over different temperature ranges to measure the interlayer probability and to separate out the two contributions to  $p$ , i.e. the prefactor ratio  $\nu_s/\nu_t$  and the step edge barrier  $\Delta E_s$  [5–9]. Results obtained from these experiments are not in full agreement [10–12]. Experiments carried out at low temperatures ( $T < 150$  K) under growth conditions indicate  $\nu_s/\nu_t > 1$  while quasi-equilibrium experiments carried out close to 300 K show  $\nu_s/\nu_t \sim 1$ . In this paper we discuss possible reasons for the discrepancy.

A distinguishing feature of the analysis of experiments carried out at the higher temperature is that they are based on a comparison of the decay rates of small adatom and vacancy islands of radius  $r$  located at the centre of larger vacancy island of radius  $R$ . It is easy to see that the small vacancy island decays over longer time than the small adatom island. One possible reason is because the diffusing atoms experience a step edge barrier at the small vacancy island but not at the edge of the small adatom island. This slows down the filling of the vacancy island and therefore its decay. For the experiments of [5] the decay rate for an  $r = 7$  nm adatom island located at the centre of an  $R = 70$  nm vacancy island is found at 300 K to be 25 times faster than the decay rate of a small vacancy located within a similar vacancy island. Such experiments were analysed under the assumption of quasi-equilibrium (i.e. steady state conditions hold) and that the detachment rate is determined thermodynamically. The step edge barrier parameters  $\Delta E_s = 0.13$  eV,  $\nu_s/\nu_t \sim 1$  and line tension  $\gamma = 0.75$  eV nm<sup>-1</sup> for Ag(111) steps were extracted. The steady state condition implies that the density of adatoms  $\rho(r')$  within the annular disc  $R \geq r' \geq r$  depends only on radius  $r'$  and is a solution to the 2D diffusion equation.

On the other hand, the terrace diffusion coefficient  $D_t$  for Ag(111) can be estimated from a different experiment as  $D_t = 2 \times 10^{11}$  s<sup>-1</sup> exp(-0.1 eV/kT) [6]. If one combines the average atom detachment rate  $E(r)$  and the terrace diffusion, under the assumption of steady state [5], then the equilibrium concentration in front of a straight step, is  $\rho_\infty = nE(r)/D_t = 0.25 \times 10^{-9}$  atoms nm<sup>-2</sup>, using the atomic density of Ag(111)  $n = 13.8$  atoms nm<sup>-2</sup>. The equilibrium concentration  $\rho_{\text{eq}}$  in front of an island of radius  $r$  is thus given by

$$\rho_{\text{eq}} = \rho_\infty \exp(\gamma/kTnr). \quad (2)$$

For the measured step energy  $\gamma = 0.75$  eV nm<sup>-1</sup>, the equilibrium concentration outside the island with  $r = 7$  nm is  $\rho_{\text{eq}}(r) = 0.33 \times 10^{-9}$  atoms nm<sup>-2</sup> and outside the vacancy island with  $R = 70$  nm is  $\rho_{\text{eq}}(R) = 0.24 \times 10^{-9}$  atoms nm<sup>-2</sup>. The difference in equilibrium concentration  $\rho_{\text{eq}}(r) - \rho_{\text{eq}}(R)$  is less than  $10^{-9}$  atoms nm<sup>-2</sup> at 300 K. If steady state conditions hold, the actual concentrations at the two boundaries at  $r$  and  $R$  deviate from the equilibrium values by less than  $10^{-10}$ , the concentration outside the small island being slightly lower and the one outside the large island slightly higher than their corresponding equilibrium values. This small difference between the actual and equilibrium concentrations provides the concentration gradient for atoms to diffuse irreversibly from the small adatom island to the larger vacancy island and for the adatom island to decay (the flow of atoms is in the opposite direction for the decay of the small vacancy island).

It is unclear whether the steady state model of analysis is applicable in the case of such small concentration differences. Further work is necessary to clarify this question. Furthermore the ratio of the detachment rates for the adatom to the vacancy island is simply determined by their curvature since this ratio is

$$E(r)/E(-R) = \rho_{\text{eq}}(r)/\rho_{\text{eq}}(-R) = \exp(\gamma/kTnr)/\exp(-\gamma/kTnR) \quad (3)$$

which is only 1.09 for the parameters of Ag(111) at 300 K. On the other hand, as will be discussed below, the energetic barriers at the island perimeter are sufficiently high. Differences in shape between the adatom (convex) and vacancy (concave) islands lead to different rate limiting processes for each case, and to a much higher ratio in their average detachment rates.

If steady state does not hold, we propose an alternative way of analysing the island decay in terms of independent atom detachment. The basic parameters are the energy barriers for the elementary processes of atom detachment from the different local environments at the island perimeter i.e. whether the atom detaches from a site on a straight step, a kink site, whether the step is A- or B-type etc. Activation energy barriers for the various processes are calculated using the nudged elastic band technique [15], which uses a series of intermediate atomic configurations (images) between well defined initial and final states before and after the barrier is crossed. These images are connected via a series of ‘elastic bands’ and the total energy of the system is minimized simultaneously to give the barrier between the two states. For an atomistic description of the system and the calculations of the total energy we have resorted to a reliable, many-body interaction potential which is based on the embedded atom method [16]. Although not as accurate as *ab initio* electronic structure calculations, these semiempirical potentials have provided a good description of the structure, energetics and dynamics of a set of fcc metal surfaces, including Ag. In the energy minimization technique all atoms in the system are allowed to relax, except where constraint is necessary for technical reasons. The model calculation system consists of  $16 \times 8$  atoms in a layer with 8 layers. The A ((100)-microfacet) or B ((111)-microfacet) type step is created by deleting about half the atoms from the top layer in the required direction. Configurations having kinks, adatoms and more than one step are created accordingly by either deleting or adding atoms.

Earlier [17] we have used simple bond counting to determine the different barriers (i.e. the coordination number of an atom in a given configuration times its nearest neighbour interaction energy). Now we estimate the corresponding energy barriers more accurately with nudged elastic band techniques. The parameters for each microscopic process are summarized in table 1. In the case of diffusion along steps, the energy barriers were published in [18, 19]. Our values are a little higher. The probabilities are compared with the faster process—diffusion on the terrace—whose probability is assumed to be 1. (We have used the calculated than the measured terrace barrier but none of the conclusions below is affected.)

Although in an earlier work [17] the probability for an atom emitted at the boundary of one of the small islands to reach either the boundary of the other island or to re-adsorb at the boundary, from which it had detached was determined. However, the actual time taken by these events was not reported. The probabilities of reaching the two boundaries (at  $r$  or  $R$  and be caught irreversibly) do not depend on the terrace diffusion coefficient, but the times to reach the boundaries do. In addition these times are needed to decide whether the assumption of steady state is justified or not. To answer this question, we have simulated the random walk of the adatoms released at  $r$  or  $R$  using a Monte Carlo method. We obtain the time for the random walk to be completed for the four possible outcomes (if an atom is released at  $r$  or  $R$  and if it is eventually caught at  $r$  or  $R$ ) measured in terms of the elementary hopping time on the terrace. These times are listed in table 2.

Inspection of tables 1 and 2 shows that the steady state condition cannot be satisfied for Ag/Ag(111) since the faster detachment time for an atom at the island boundary ( $P_{3B}$  process) is  $10^4$  larger than the longer hopping time in the annular region between the islands.

An alternative way to analyse the island decay experiments is in terms of the independent detachment model to deduce the prefactor ratio  $\nu_s/\nu_t$ . For the island boundary we use the island shapes extracted experimentally in [14] and shown schematically in figure 1. The island boundary consists of kinked and straight segments of approximately equal length. For the

**Table 1.** Energy barriers and relative probabilities of microscopic processes on steps.

Process	Energy barrier $\Delta E$ (eV)	Relative probability at $T = 150$ K	Relative probability at $T = 300$ K
$P_0$ —diffusion on the terrace	0.061	1	1
$P_{1A}$ —detachment from straight step A	0.758	$5.3 \times 10^{-24}$	$2.3 \times 10^{-12}$
$P_{1B}$ —detachment from straight step B	0.691	$9.2 \times 10^{-22}$	$3.0 \times 10^{-11}$
$P_{2A}$ —diffusion along step A	0.294	$1.7 \times 10^{-8}$	$1.3 \times 10^{-4}$
$P_{2B}$ —diffusion along step B	0.338	$5.6 \times 10^{-10}$	$2.3 \times 10^{-5}$
$P_{3A}$ —detachment of kink site on A step	0.571	$9.3 \times 10^{-18}$	$3.1 \times 10^{-9}$
$P_{3B}$ —detachment of kink site on B step	0.527	$2.7 \times 10^{-16}$	$1.6 \times 10^{-8}$
$P_{4A}$ —rounding kink position on A step	0.570	$1.0 \times 10^{-18}$	$3.1 \times 10^{-9}$
$P_{4B}$ —rounding kink position on B step	0.582	$4.0 \times 10^{-18}$	$2.1 \times 10^{-9}$
$P_{5A}$ —detachment of kink position to the straight segment of the A step	0.471	$2.0 \times 10^{-14}$	$1.4 \times 10^{-7}$
$P_{5B}$ —detachment of kink position to the straight segment of the B step	0.540	$1.0 \times 10^{-16}$	$1.0 \times 10^{-8}$

**Table 2.** The mean number of jumps to reach the appropriate boundary.

Diffusion from boundary to boundary	Mean number of jumps
$r \rightarrow R$	$3 \times 10^4$
$r \rightarrow r$	$5 \times 10^2$
$R \rightarrow r$	$\sim 10^6$
$R \rightarrow R$	$2 \times 10^2$

adatom island we assume that all the atoms at the kinked segments evaporate first, within  $\tau_k$  (the time for a kink atom i.e. an atom with three nearest neighbours), since the atoms at the kinked segment detach independently. Once these atoms detach, then atoms from the straight segments follow sequentially, since the corner atoms at the straight segments (which also have 3 nearest neighbours) need to detach before the neighbouring straight step atom becomes a kink atom with 3 neighbours. The straight segment proceeds to ‘unzip’ in time  $(n_s/2)\tau_k$  with  $n_s$  the number of atoms at the straight segment, since there are two corner atoms to initiate the ‘unzipping’. The asymmetry between concave and convex island shapes can be best illustrated if we express the barriers in terms of an effective nearest neighbour interaction energy  $\varepsilon$ . For the initial adatom island,  $r = 7$  nm, we have  $n_s = 12$  so the average detachment time from the adatom island is

$$\tau_a = (1 + n_s/2)\tau_k = 7\tau_k, \quad (4)$$

where

$$\tau_k = \nu^{-1} \exp(3\varepsilon/kT) \quad (5)$$

is the time to detach from a kink site.

Similarly we find the average time  $\tau_v$  for an atom to detach from the larger vacancy island  $R = 70$  nm. In the independent detachment model, this time determines the decay of the smaller vacancy island, since the released atoms, diffuse ‘instantaneously’ to refill the smaller vacancy island at  $r$ . This process is schematically shown in figure 2. As argued before, first the atoms at the kinked segments detach within  $\tau_k$ . Although there are equilibrium fluctuations

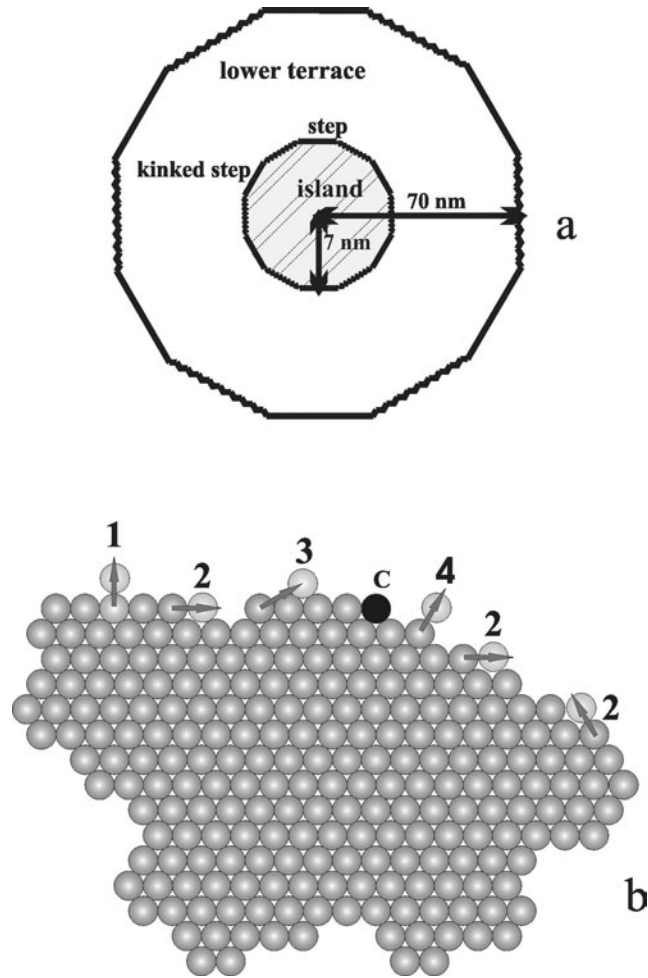


**Figure 1.** Illustration of an adatom island decay geometry. (a) The island shape has kinked and straight segments as found in [14]. In the middle of a large vacancy island of radius  $R$  initially an adatom island of radius  $r$  is present. The height of the small island is the same as the surrounding region of the vacancy island. (b) The processes on the island edge: 1—detachment from straight segment ( $P_{1A}, P_{1B}$ ), 2—diffusion along step ( $P_{2A}, P_{2B}$ ), 3—kink rounding ( $P_{4A}, P_{4B}$ ) and 4—kink detachment ( $P_{3A}, P_{3B}$ ). Atom  $c$  is a corner atom with 3 bonds.

at the straight segments at finite temperatures which can generate kinks, these kinks cannot account for the decay of the island under the non-equilibrium conditions assumed in the independent detachment model, which is based on the irreversible decay of the island. For an atom to detach it is necessary for two sequential processes to occur: first the generation of the kink atoms (as in equilibrium) with barrier  $2\varepsilon$  (where  $\varepsilon$  is the nearest neighbour interaction energy), and, in addition, the same atom detaches to the terrace by breaking two bonds so the combined process will have a total barrier  $\varepsilon_t = 2\varepsilon + 2\varepsilon = 4\varepsilon$ . The time needed for this process is approximated

$$\tau = v^{-1} \exp(4\varepsilon/kT) = \exp(\varepsilon/kT)\tau_k. \quad (6)$$

This proves the essential asymmetry between the decay of the vacancy and adatom islands. The corner atoms at a vacancy island have five nearest neighbours so they cannot initiate the

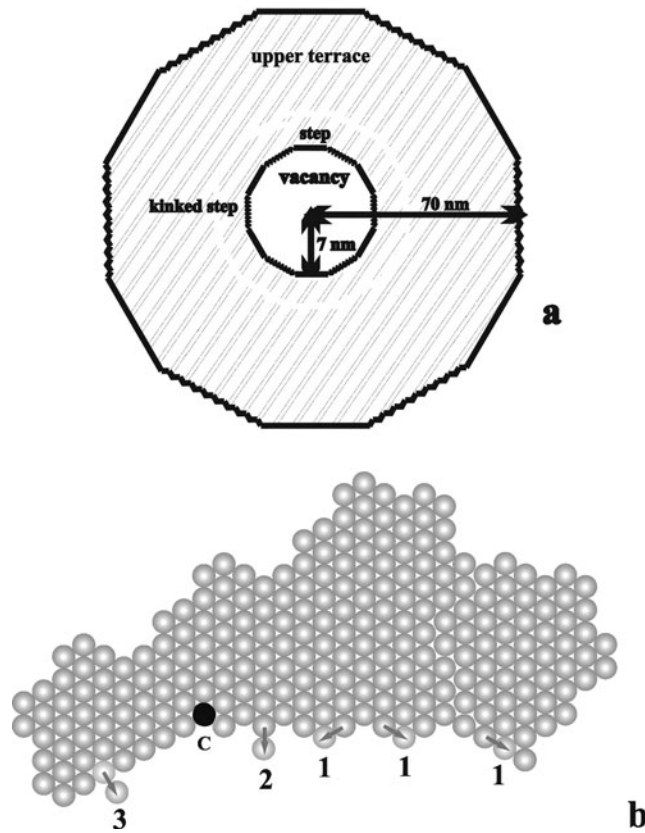


**Figure 2.** Illustration of a vacancy island decay geometry. (a) The island shape has kinked and straight segments as found in [14]. In the middle of a large vacancy island of radius  $R$  a small vacancy island of radius  $r$  is initially created. The height of the small vacancy island is two layers lower than the surrounding region of the large vacancy island. (b) The processes on the vacancy island edge: 1—diffusion along step ( $P_{2A}$ ,  $P_{2B}$ ), 2—kink detachment ( $P_{3A}$ ,  $P_{3B}$ ) and 3—detachment from straight segment ( $P_{1A}$ ,  $P_{1B}$ ). Atom  $c$  is a corner atom with 5 bonds.

‘unzipping’ as in the adatom island. An atom at a straight step needs to detach with a higher barrier (as shown in equation (6)) to generate a kink. Since it is known experimentally that the shape of the islands remains unchanged (presumably because of the very fast edge diffusion around the perimeter), it is not possible to have all the successive kinked rows detaching before atoms of the straight edge detach. Besides, the number of atoms available within the six triangular kinked regions is only around 100 atoms while the refilling of the small vacancy island requires more than 1200 atoms. So there is a need for atoms at the straight segment to detach and generate the kinked atoms.

Assuming the vacancy island shape to be the one of figure 2(a), since as seen in experiments it remains unchanged, the kink atom can be generated anywhere on the straight edge, so the ‘unzipping’ involves  $n$  atoms (with  $n_s/2 < n < n_s$ ). The average time it will take the straight segment to ‘unzip’ will be  $(3/4n'_s)\tau_k$ . Since these processes happen successively, the total time will be

$$\tau_v = (1 + \exp(\varepsilon/kT) + (3/4n'_s))\tau_k. \quad (7)$$

For  $R = 70$  nm,  $n'_s = 120$ ,  $\varepsilon = 0.2$  eV [5], comparable to the calculated barriers of table 1 in the range 0.15–0.19 eV, we have  $\tau_v = 2400\tau_k$ . These times need to be averaged over the total

number of atoms emitted since the perimeter of the larger vacancy island involves more atoms than the perimeter of the small adatom island. The detachment rates of the islands,  $E(r)$  and  $E(-R)$ , are the mean average number of atoms detached per unit of time.

$$E(r) = \frac{2\pi r}{a} \frac{1}{\tau_a}, \quad E(-R) = \frac{2\pi R}{a} \frac{1}{\tau_v}, \quad (8)$$

where  $a$  is the lattice constant. The ratio of detachment rates:

$$E(r)/E(-R) = (r/R)\tau_v/\tau_a \approx 35, \quad (9)$$

much larger than the ratio 1.09, from (3), for steady state model (where  $\gamma = 0.75 \text{ eV nm}^{-1}$  [5]).

We can now write expressions for the adatom and vacancy island decay rates within the independent detachment model. For the adatom island:

$$n \frac{dA_a}{dt} = \frac{2\pi r}{a} E(r) P_r - \frac{2\pi R}{a} E(-R) P_R \approx \frac{2\pi r}{a} E(r) P_r \quad (10)$$

where  $A_a$  is the area of an adatom island,  $n = 13.8 \text{ atoms nm}^{-2}$  is two-dimensional density of Ag(111) and

$$P_r = c/(r \ln r/a) \quad (11)$$

is the probability of an atom detached from the island at  $r$  to reach the boundary at  $R$ .

$$P_R = c/(R \ln(R/a)) \quad (12)$$

is the similar value for the atoms detached at  $R$  to reach the island boundary at  $r$  ( $c$  is constant which normalizes the probability). According to relations (9), (11) and (12),  $rE(r)P_r \gg RE(-R)P_R$ , so we can neglect the second term in the right-hand side of equation (10).

Similar for the vacancy island

$$n \frac{dA_v}{dt} = \frac{2\pi R}{a} E(-R) P_{R_s} \quad (13)$$

where  $A_v$  is the area of a vacancy island and the probability for an atom detached at  $R$  to be adsorbed at  $r$  after overcoming the reflecting boundary [13] is given by:

$$P_{R_s} = (c/(R \ln R/a))(p/(1 - (1 - p)(1 - P_r))). \quad (14)$$

Within our model we can express the ratio of the decay rates of the adatom and vacancy islands in terms of the averaged detachment times. Using (8) we obtain

$$(dA_a/dt)/(dA_v/dt) = (P_r/P_{R_s})(r/R)^2 \tau_v/\tau_a. \quad (15)$$

Using the data for adatom versus vacancy island decay of Ag/Ag(111) at  $T = 300 \text{ K}$ ,  $r = 7 \text{ nm}$ ,  $R = 70 \text{ nm}$ ,  $\Delta E_s = 0.13 \text{ eV}$ ,  $\tau_v/\tau_a = 35$ ,  $(dA_a/dt)/(dA_v/dt) = 25$ , we obtain  $p \gg P_{R_s}$  which implies  $\nu_s/\nu_t > 30$ . This brings the value of the prefactor ratio in close agreement with the low temperature growth experiments.

## 2. Conclusions

Because of the large difference between the atom detachment and atom terrace diffusion rates for Ag/Ag(111), we have presented an alternative interpretation of the island versus vacancy decay experiments. Within this interpretation the decay process consists of independent atom detachments, instead of continuous atom emission under steady conditions. With the new analysis one obtains  $p \gg P_{R_s}$ , which implies  $\nu_s/\nu_t > 30$  and a better agreement between the high and low temperature experiments. However further work is needed to specify detailed experimental criteria for deciding the range of validity of the independent versus steady state model in island decay experiments.



## Acknowledgments

Ames Laboratory is operated for the US Department of Energy by Iowa State University under Contract No W-7405-Eng-82. ZC acknowledges financial support from grant No IAA1010207 of the Grant Agency of Academy of Sciences of the Czech Republic. The work of TSR and CG was supported partially by NSF under grant EEC0085604.

## References

- [1] Tringides M C (ed) 1997 *Surface Diffusion: Atomistic and Collective Processes* (New York: Plenum)
- [2] Stanley M, Papageorgopoulos C, Ross K R and Tringides M C 1996 *Surf. Sci.* **335** L264
- [3] Rosenfeld G, Servanty R, Teichert C, Polsema B and Comsa G 1993 *Phys. Rev. Lett.* **72** 895
- [4] Vrijmoeth J, van der Vegt H A, Meyer J A, Vlieg E and Behm R J 1994 *Phys. Rev. Lett.* **72** 383
- [5] Morgenstern K, Rosenfeld G, Laegsgaard E, Besenbacher F and Comsa G 1998 *Phys. Rev. Lett.* **80** 556  
Rosenfeld G *et al* 1998 *Surf. Sci.* **402–404** 401
- [6] Bromann K, Brune H, Roder H and Kern K 1995 *Phys. Rev. Lett.* **75** 677
- [7] Ross K R and Tringides M C 1998 *Surf. Sci. Rev. Lett.* **5** 833
- [8] Ross K R and Tringides M C 2000 *Phys. Rev. Lett.* **85** 1480
- [9] Meyer J A, Vrijmoeth J, van der Vegt H A, Vlieg E and Behm R J 1995 *Phys. Rev. B* **51** 14790
- [10] Morgenstern K and Besenbacher F 2001 *Phys. Rev. Lett.* **87** 149602
- [11] Ross K R and Tringides M C 2001 *Phys. Rev. Lett.* **87** 149604
- [12] Ross K R and Tringides M C 2001 *Phys. Rev. Lett.* **87** 149606
- [13] Rosenfeld G, Morgenstern K and Comsa G 1997 *Surface Diffusion: Atomistic and Collective Processes* ed M C Tringides (New York: Plenum) p 361
- [14] Steimer Ch, Giesen M, Verheij L and Ibach H 2001 *Phys. Rev. B* **64** 085416-1
- [15] Jonsson H, Mills G and Jacobsen K W 1998 Nudged elastic band method for finding minimum energy paths of transitions *Classical and Quantum Dynamics in Condensed Phase Simulations* ed B J Berne, G Ciccotti and D F Coker (Singapore: World Scientific)
- [16] Foiles S M, Baskes M I and Daw M S 1986 *Phys. Rev. B* **33** 7983
- [17] Chvoj Z and Tringides M C 2002 *Phys. Rev. B* **66** 035419
- [18] Ferrando R and Treglia G 1994 *Phys. Rev. B* **50** 12104
- [19] Ala-Nissila T, Ferrando R and Ying S C 2002 *Adv. Phys.* **51** 949